Density Functional Theory Analysis of the Impact of Steric Interaction on the Function of Switchable Polarity Solvents

ARTICLE *in* THE JOURNAL OF PHYSICAL CHEMISTRY B · MAY 2015

Impact Factor: 3.3 · DOI: 10.1021/acs.jpcb.5b03167 · Source: PubMed

4 AUTHORS, INCLUDING:

Aaron D. Wilson
Idaho National Laboratory
21 PUBLICATIONS **865** CITATIONS

SEE PROFILE

THE JOURNAL OF PHYSICAL CHEMISTRY B

Article

pubs.acs.org/JPCB

Density Functional Theory Analysis of the Impact of Steric Interaction on the Function of Switchable Polarity Solvents

Joshua S. McNally,[†] Bruce Noll,[‡] Christopher J. Orme,[†] and Aaron D. Wilson*,[†]

[†]Idaho National Laboratory, P.O. Box 1625 MS 3732, Idaho Falls, Idaho 83415-3531, United States

[‡]Bruker AXS Inc., 5465 East Cheryl Parkway, Madison, Wisconsin 53711, United States

Supporting Information

ABSTRACT: A density functional theory (DFT) analysis has been performed to explore the impact of steric interactions on the function of switchable polarity solvents (SPS) and their implications on a quantitative structure−activity relationship (QSAR) model previously proposed for SPS. An X-ray crystal structure of the *N*,*N*-dimethylcyclohexylammonium bicarbonate (Hdmcha) salt has been solved as an asymmetric unit containing two cation/anion pairs, with a hydrogen bonding interaction observed between the bicarbonate anions, as well as between the cation and anion in each pair. DFT calculations provide an optimized structure of Hdmcha that closely resembles experimental data and reproduces the cation/anion interaction with the inclusion of a dielectric field. Relaxed potential energy surface (PES) scans have been performed on Hdmcha-based computational model compounds, differing in the size of functional group bonded to the nitrogen center, to assess the steric impact of the group on the relative energy and structural properties of the compound. Results suggest that both the length and amount of branching associated with the substituent impact the energetic limitations on rotation of the group along the N−R bond and NC−R bond, and disrupt the energy minimized position of the hydrogen bonded bicarbonate group. The largest interaction resulted from functional groups that featured five bonds between the ammonium proton and a proton on a functional group with the freedom of rotation to form a pseudo six membered ring which included both protons.

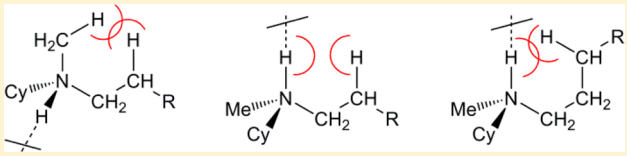

1. INTRODUCTION

Switchable polarity solvents (SPS) have recently become an area of interest for a variety of potential applications, including extractions (algal,[1−5] biomass,[6] and oil sands[7]), biomass pretreatment and fractionation,[8,9] pyrolysis oil fractionation,[10] carbon capture,[11−16] reaction media, and osmotically driven membrane processes (ODMP),[17−19] including water treatment and osmotic heat engines. In particular, the use of SPS as a draw solute has recently been demonstrated for the purification of water using a forward osmosis process.[20] This class of solvents is capable of switching between an aprotic nonionic form, to a water-soluble ionic liquid/solute through the introduction and removal of CO_2 (eq 1).

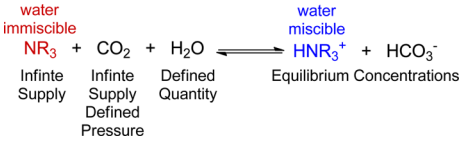

Dimethylcyclohexylamine (dmcha) has been demonstrated as the premiere switchable polarity solvent and highlights the importance of ring systems in the functionality of SPS.[2,6,7,10,17,18,21,22] For this reason, there is interest in the electronic and structural properties exhibited by dmcha that dictate its reaction mechanisms, and describe its function as a SPS. The development of a knowledge base describing these properties will allow for predictive studies focused on the use of different SPS-amines for the large variety of applications listed above. A previous study from our lab screened a variety of tertiary amines for their ability to function as SPS, as well as their ability to produce an osmotic flux across a semipermeable membrane.[18] It was found that a C:N ratio between 6 and 12 is necessary for an amine to act as a SPS, and that the amine:carbonate ratio in its polar form is an important factor in terms of its osmotic properties. In addition, this work led to the development of a model in which molecular structure of the amine is correlated with the maximum equilibrium concentration a SPS achieves when a fixed volume of water is exposed to an unlimited supply of amine and CO_2 at a given pressure (eq 1). In the previous paper the model was referred to as a structure−function model; however, to remain consistent with broader areas of research, it will be subsequently referred to as the quantitative structure−activity relationship (QSAR) model.[18] This QSAR model serves as one of two models that have been published to better predict the function of SPS and advance their application. As an alternative, Jessop et al. developed a model (pK_a/K_{OW} model) which correlates a predictive combinatorial equilibrium dimension on a graph featuring a range of organic ammonium pK_as and aqueous organic partition coefficients K_{OW}.[21,22]

The pK_a/K_{OW} model focuses on developing SPS for organic extractions and in doing so highlights the need to balance the

Received: April 1, 2015
Revised: April 29, 2015
Published: May 4, 2015

DOI: 10.1021/acs.jpcb.5b03167
J. Phys. Chem. B 2015, 119, 6766−6775

polarity of the SPS to achieve good switching as well as good isolation of the organic product. The pK_a/K_{OW} model must make approximations such as assuming aqueous pK_as and aqueous Henry's law constants. Such values are solvent dependent, but in their concentrated polar form, SPS deviate significantly from a strictly aqueous solution. This deviation is demonstrated by nonosmotic SPS and solubility of the neutral amine in osmotic SPS.[18] Performance metrics based on such approximate solvent dependent values can provide gross estimates, but finer predictions are not possible. An example of where the pK_a/K_{OW} model breaks down is Hünig's base ($N(iso\text{-}Pr)_2Et$). According to the pK_a/K_{OW} model, the pK_a (11.4) and K_{OW} (2.3) of Hünig's base could/should make an optimal two liquid SPS.[22] In contrast to this prediction Hünig's base does not function as a SPS at ambient conditions.

Hünig's base epitomizes how molecular structure impacts SPS function differently than is captured by pK_a and K_{OW}. The QSAR model is premised on steric bulk near the nitrogen lone pair reducing SPS performance. In this frame of reference, the well-studied low nucleophility of Hünig's base is more relevant than its pK_a. Hünig's base is still a challenge for the first iteration of the QSAR model, which incorrectly predicts it to be a SPS, albeit a poorly performing SPS. In an effort to further develop our understanding of the importance of steric bulk in the performance of tertiary amines as SPS, DFT studies were performed on a series of model compounds differing in their amine substituents. The studies presented in this paper consider the energy barriers associated with the rotation of each functional group about the N−R and NC−R bond, as well as the disruption to the position of the hydrogen-bonded bicarbonate group caused by the rotation of the substituent. The geometry optimized properties of dimethylcyclohexylammonium bicarbonate are compared to the crystallographic data of the salt, presented herein, along with a discussion regarding the potential for solution state ion pairing similar to what is observed in the solid state crystal structure.

2. EXPERIMENTAL SECTION

2.1. Crystallographic Analysis. Crystals of dimethylcyclohexylammonium bicarbonate (Hdmcha, Figure 1) were

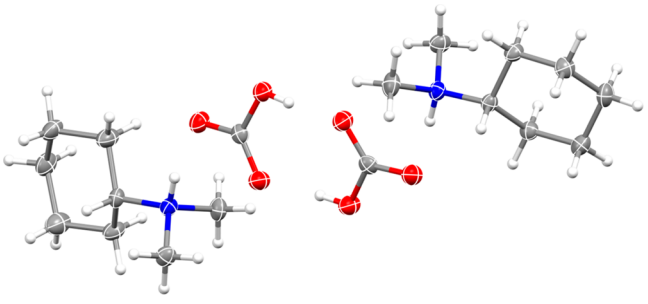

Figure 1. Hdmcha asymmetric dimer unit. Color scheme: red = oxygen; blue = nitrogen; gray = carbon; white = hydrogen.

obtained by mixing deionized water (154.32 g, 8.57 mol) with dimethylcyclohexylamine (321.30 g, 2.52 mol). A mass flow controller was used to deliver CO_2 to the mixture at 80−110 mL/min for 5 periods of 7−10 h.[18] From this reaction mixture, clear colorless crystals of Hdmcha grew over a period of 2 days. X-ray data was collected on a Bruker D8 QUEST diffractometer system (Bruker AXS Inc.) equipped with a curved graphite monochromator and a 0.71072 Å Mo Kα sealed tube. The frames were integrated with the Bruker SAINT software package using a narrow-frame algorithm, and data were corrected for absorption effects using the multiscan method (SADABS). The structure was solved and refined using the Bruker SHELXTL software package. The final anisotropic full-matrix least-squares refinement on F-squared with 249 variables converged at R_1 = 3.86%. Pertinent crystallographic details can be found in Tables 1 and 2.

Table 1. Data Collection and Structure Refinement for Hdmcha

diffractometer	Bruker D8 QUEST diffractometer
radiation source	sealed tube, Mo Kα
θ range for data collection	3.09° to 28.28°
index ranges	$-22 \le h \le 22$, $-14 \le k \le 13$, $-14 \le l \le 13$
reflns collected	30684
indep corrections	4975 [R_{int} = 0.0446]
coverage of indep reflections	99.8%
abs correction	multiscan
max and min transm	0.9900 and 0.9760
struct soln technique	Direct methods
struct soln program	SHELXT v2014/1 (Sheldrick, 2014)
refinement meth	Full-matrix least-squares on F^2
refinement program	SHELXL-2013 (Sheldrick, 2013)
function minimized	$\Sigma\, w(F_o^2 - F_c^2)^2$
data/restraints/params	4975/0/249
goodness-of-fit on F^2	1.017
final R indices	3934 data; $I > 2\sigma(I)$, R1 = 0.0386, wR2 = 0.0864
	all data; R1 = 0.0563, wR2 = 0.0944
weighting scheme	$w = 1/[\sigma^2(F_o^2) + (0.0449P)^2 + 0.5619P]$ where $P = (F_o^2 + 2F_c^2)/3$
largest diff peak and hole	0.372 and −0.207 e Å^{-3}
rms deviation from mean	0.046 e Å^{-3}

2.2. Computational Methodology. All geometry optimizations and vibrational frequency calculations were carried

Table 2. Sample and Crystal Data for Hdmcha

identification code	dimethylcyclohexylammonium bicarbonate
chem formula	$C_9H_{19}NO_3$
formula wt	189.25
temp	100(2) K
wavelength	0.71073 Å
cryst size	0.105 × 0.140 × 0.265 mm
cryst habit	clear colorless triangular prism
cryst syst	monoclinic
space group	$P\ 1\ 2_1/c\ 1$
unit cell dimens	a = 16.8512(10) Å
	b = 11.1738(8) Å
	c = 11.0083(8) Å
	α = 90°
	β = 104.138(3)°
	γ = 90°
vol	2010.0(2) Å^3
Z	8
density (calcd)	1.251 g/cm^3
abs coeff	0.093 mm^{-1}
F(000)	832

DOI: 10.1021/acs.jpcb.5b03167
J. Phys. Chem. B 2015, 119, 6766−6775

out using Gaussian03 (Revision C.02).[23] The B3LYP functional, which uses Becke's three parameter exchange functional (B3) and the correlation function of Lee, Yang, and Parr (LYP),[24−29] was used for all calculations. The valence triple-ζ 6-311++G(d,p) basis set was used, which includes polarization functions on all atoms and diffuse functions on non-hydrogen atoms. Frequency calculations performed at the B3LYP/6-311++G(d,p) level of theory confirmed energy minimized geometries with the absence of any imaginary frequencies. Potential energy surface scan calculations were performed at the B3LYP/6-311++G(d,p) level of theory.

The geometric parameters associated with **1a** (Figure 2) were obtained from the X-ray crystal structure data, which was

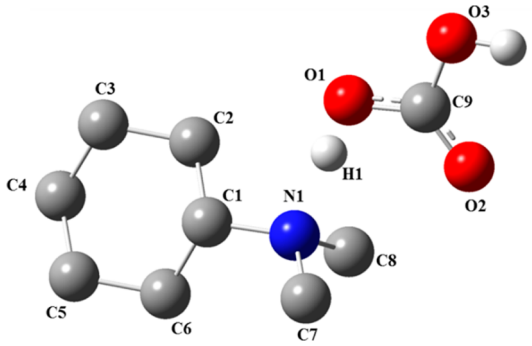

Figure 2. Geometry optimized **1a**. Select hydrogen atoms have been removed for clarity.

solved as an asymmetric unit containing two pairs of the cation and anion (*vide infra*). The parameters of a single pair were geometry optimized to give an energy minimized structure of **1a**. The initial geometries of the remaining theoretical amines (**2a−c**, **3a−c**, and **4a**), with an overall N(R)MeCy skeleton structure, were generated using Gaussview (Revision 3.09). Relaxed potential energy surface scans were performed using Gaussian03 with the dihedral angles associated with the atoms in question for each configuration being incrementally adjusted, and the energy being calculated at each point. **1a** was also geometry optimized with a solvent model (H_2O, dielectric constant = 78.4) using the self-consistent reaction field (SCRF) calculation as implemented by Gaussian03 with IEF-PCM.

3. RESULTS AND DISCUSSION

In the continued effort to develop SPS systems for use in processing, extraction, and separation technologies, an understanding of the structural properties that limit or affect the ability of a tertiary amine to function as a SPS is necessary. A QSAR model has been proposed to help provide insight into the differences in SPS behavior exhibited by a variety of tertiary amines. This QSAR model intends to specifically predict the equilibrium concentration of the polar form of individual SPS rather than suggest potential performance. To further explore SPS performance, it is reasonable to start with what is arguably the most effective SPS, dimethylcyclohexylamine.[6,18] Upon reaction with CO_2, the resulting salt, dimethylcyclohexylammonium bicarbonate, reaches the highest known concentration of any characterized SPS in terms of weight percent (77 wt %), molality (18.0 mol/kg by amine), and molarity (4.6 M by amine). Its structure is optimal to form a concentrated polar tertiary ammonium bicarbonate solution. We recently discovered that the fully saturated solution of 77 wt % dimethylcyclohexylammonium bicarbonate solution ([HN(Me)$_2$CyHCO$_3$·3H$_2$O]) forms a crystalline dimer of Hdmcha. The resulting crystal structure serves as an ideal starting point for a computational investigation of SPS function.

3.1. Crystallographic Analysis and DFT Comparison.

The X-ray crystal structure of Hdmcha shows an asymmetric unit containing two cation/anion pairs (Figure 1). A hydrogen bonding interaction is observed between the bicarbonate anions, which forms the dimer. In each pair, there is a hydrogen bond between the donor H atom of the ammonium and an acceptor oxygen atom of the bicarbonate.

As can be seen in Figure 1 and Table 3, the refined structure shows a hydrogen bond interaction, with a protonated ammonium cation, and deprotonated bicarbonate anion, with an N1−O1 bond of 2.65 Å. The placement and associated bond distances of the hydrogen atom in the crystal structure refinement (Hdmcha) were made according to calculated geometries and associate the proton with the nitrogen (N1−H1 = 0.90 Å and O1−H1 = 1.76 Å). This position of the proton (H1) is consistent with chemical shifts observed in solution state NMR.[18]

A DFT optimized structure of one of the ammonium bicarbonate pairs was obtained using parameters from the

Table 3. Select Bond Lengths and Angles for the Hdmcha Crystal Structure and 1a, Both with and without PCM[a]

bond	Hdmcha	1a	1a PCM	angle	Hdmcha	1a	1a PCM
N1−H1	0.90	1.61	1.07	N1−C1−C2	111	112	111
N1−C1	1.52	1.49	1.53	C2−C3−C4	110	111	111
C1−C2	1.52	1.54	1.53	C3−C4−C5	112	112	111
C2−C3	1.53	1.54	1.54	C4−C5−C6	111	111	112
C3−C4	1.53	1.53	1.53	C5−C6−C1	109	111	110
C4−C5	1.52	1.53	1.53	C6−C1−N1	113	115	113
C5−C6	1.53	1.54	1.54	C7−N1−C8	110	110	110
C1−C6	1.52	1.54	1.53	C1−N1−H1	108	108	106
N1−C7	1.49	1.47	1.49	O1−C9−O2	125	127	128
N1−C8	1.49	1.47	1.49	O1−C9−O3	115	110	114
O1−H1	1.76	1.04	1.60	O2−C9−O3	120	123	119
C9−O1	1.26	1.31	1.27				
C9−O2	1.26	1.22	1.24				
C9−O3	1.35	1.35	1.38				
N1---O1	2.65	2.65	2.67				

[a]See Figure 2 for atom labels.

DOI: 10.1021/acs.jpcb.5b03167
J. Phys. Chem. B 2015, 119, 6766−6775

crystallographic data as input. As shown in Figure 2 and Table 3, the optimized configuration (**1a**) shares many geometric properties with Hdmcha, with the majority of bond lengths and angles being quite similar. However, there is difference in the bond lengths associated with the N1−H1−O1 hydrogen bonding interaction. Again, the placement and bond distance of the hydrogen atom in the crystal structure refinement (Hdmcha) were made according to calculated geometries and associate the proton with the nitrogen (N1−H1 bond (0.90 Å)). In **1a**, the hydrogen atom is more closely associated with the bicarbonate oxygen (O1−H1 bond 1.04 Å). Thus, the ionic nature of the interaction is not accurately represented in the DFT structure **1a**, where the ammonium and bicarbonate ions are better described as neutral ammonia and carbonic acid species. However, the N1−O1 bond length is the same (2.65 Å) in the crystal structure, Hdmcha, and the optimized structure, **1a**. To better simulate the higher effective dielectric constant present in the crystal lattice that the gas-phase model does not account for, **1a** was geometry optimized with a polarized continuum model (PCM), using H_2O as the solvent to yield **1a PCM**. As shown in Table 3, the presence of a dielectric field used with **1a PCM** provides a geometry reflecting the cation−anion interaction modeled in the crystal structure, with a shorter N1−H1 bond (1.07 Å) and a longer O1−H1 bond (1.60 Å). The N1−O1 bond length is still very similar to the crystal structure data (2.67 vs 2.65 Å). The DFT analysis described herein is concerned with geometric properties and steric effects associated with different functional groups, so the position of the hydrogen atom in the hydrogen bond and the overall ionic character of the system are not important. Because the bicarbonate group is bonded to the amine at the correct distance in the structure of **1a** without a dielectric field included, it was determined that the remainder of the computational studies would be carried out without implementing PCM to reduce the overall computational expense.

3.2. Freezing-Point Evidence for Solution State Ion Pairing. The crystal structure data is important as a starting point for computational analysis; however, as a solid state structure, the relevance of the ion pairing shown in the data to the solution state is not necessarily implied. The DFT results discussed in the previous section very closely reproduce the crystal structure data, particularly with the implementation of the PCM model. Ion pairing is directly relevant to the solution state and can be investigated through colligative properties. Though the exact state of the system in solution is not entirely understood, previous studies[18,19] have provided solution state data that can allow a preliminary inference into the nature of the solution. The ratio of amine to carbonic acid in Hdmcha is not 1:1 but rather ∼1:1.06, which complicates the following van't Hoff index analysis. In contrast, cyclohexylpiperidine (CHP) has a clear 1:1 relationship, which is simpler to present and yields results that are very similar. A van't Hoff index of 1.79 has been previously reported for CHP based on freezing point data.[19] This van't Hoff index is a composite of information related to ion pairing, waters of hydration, and a minor amount of information related to a density correction. Each of these components can be quantitatively addressed: the waters of hydration (which increases the uncorrected composite van't Hoff index), ion pairing (which reduces the composite van't Hoff index), and density correction (which increases the uncorrected composite van't Hoff index).

The density correction is required to reconcile the molal concentration (mol/mass solute to mass solvent ratio) to the units used in the Morse equation. These units are based on the semiempirical semitheoretical nature of its predecessor, the van't Hoff equation. The density correction should convert the molal (mol/kg) solvent mass to either the solvent volume or solution volume. If the correction is to the solvent volume, then it would require the density of water or, more likely, the partial molar density of the water, which is very close to water but impossible to separate from the partial molar density of the solute. If the conversion was to go from solvent to solution, the corrected concentration would increase in turn, reducing the van't Hoff index significantly. It is not clear which correction is correct: the solvent density, the solvent's partial molar density, or the solution density. However, for the current analysis, the correction does not impact the result as long as the hydration correction is allowed to vary. With a floating hydration correction, the same ion pairing is approximated regardless of the density correction. Applying the largest density correction (solution density) suggests even more ion pairing, which only strengthens the subsequent arguments. What follows ignores the density correction (or assumes a solvent density conversion of 1 kg/L), which is the most conservative approach relative to approximating the degree of ion pairing.

The hydration numbers of tertiary amines are not well published; however it is likely between the hydration of a proton and an ammonium ion. It has been reported that a proton has ∼6.7 waters of hydration and ammonium has ∼1.8 waters of hydration.[30,31] Applying these hydration numbers to the cyclohexylpiperidine data results in a "waters of hydration corrected" van't Hoff index, i_{hc}, between 1.37 and 1.67 with the van't Hoff plot reaching maximum linearity at ∼3.3 waters of hydration and a van't Hoff index of 1.58 (Figure 3).

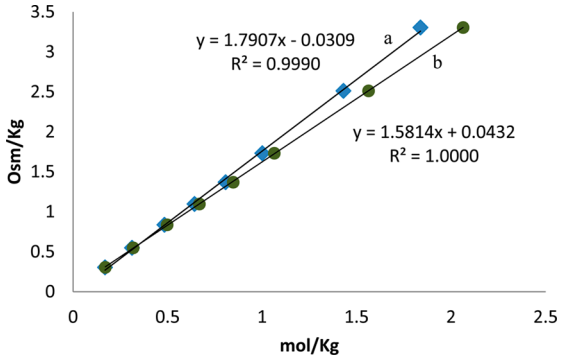

Figure 3. Observed freezing point osmolality plotted against amine concentration for amine bicarbonate solutions of CHP unmodified (i = 1.79, plot a) and CHP with concentration corrected for 3.3 waters of hydration (i_{hc} = 1.48, plot b).

Once corrected for waters of hydration, a full dissociation of ions would predict an i_{hc} of 2, accounting for complete ion independence. If the solution state featured perfect first order ion pairing, one cation interacting with one anion (without a higher order equilibrium involving multiple cations and/or multiple anions), then an i_{hc} of 1 would be expected. Intermediate states are illustrated by eq 2, where conceptually a fraction of the ions are paired $(1 - x)$ and a fraction (x) are independent.

$$i_{hc} = (1 - x)\mathrm{AB} + (x)\mathrm{A}^+ + (x)\mathrm{B}^- = 1 + x \qquad (2)$$

DOI: 10.1021/acs.jpcb.5b03167
J. Phys. Chem. B 2015, 119, 6766−6775

Assuming binary states of paired and unpaired as implied by eq 2 is a highly reduced model of the data. While it is possible that there are two states (hydrogen bond or no hydrogen bond), there may also be a spectrum of states based on Coulombic pairing and defined by a range of distances between paired and unpaired. It may be more appropriate to imagine an ion-pair character ($1 - x$ in eq 2) as the summation of a distribution of fluxional interion states for all ions in solution ranging from fully independent to fully paired. Regardless of the model, an observed i_{hc} of 1.58 implies 42% ion-pairing character for CHP. When this analysis is done for Hdmcha, an ion-pairing character is found to be ~50%. A significant portion (if not all) of the 43−50% ion-pairing character is expected to involve the bicarbonate anion associated with the ammonium cation through a hydrogen bond, which is consistent with other protic ionic liquids (PIL).[32]

Previously published data from our lab identified that, when the carbonate anion is not associated, there is likely a tightly bonded hydration environment.[18,33] It was suggested that this hydration sphere required a steric environment which is supported by significant steric impacts on entropic stability of $BH^+ \cdot H_2O$ complexes.[34] The impact of these entropic effects may be mitigated by the fluxional nature of hydration spheres, which are known to rearrange very quickly, and may be able to adapt to the steric disturbances under consideration. Many amines that can form PILs with strong acids cannot form a stable ammonium bicarbonate solution of an appreciable concentration. The adaptability of the hydration sphere could explain why a given amine and strong acid can form a neat PIL. An open steric environment apparently is not required for protons of a strong acid but is required for weak acids where hydrogen bond based ion pairing is necessary to achieve high equilibrium concentrations.

3.3. Potential Energy Surface (PES) Scan Method of Functional Group Steric Effects of Model Compounds. A DFT analysis was performed to study the steric effects associated with various functional groups. As stated, the performance of an amine as a SPS has been found to correlate with its ability to form high equilibrium concentrations in its polar form (eq 1). It follows that a strong interaction between the polar, ionic pair is a necessary component of the function of an amine as a SPS. Larger functional groups would be expected to prevent the assembly of solvent and counterion pairs, which stabilize the polar form of the SPS. A previous study[34] suggested increased entropy effects with increasing steric crowding due to the hindrance of internal rotors in the ion pairs or hydrated ions.

To gain insight into the potential steric impact imposed by the functional groups bonded to a switchable polarity solvent, potential energy surface (PES) scans were performed, and the energies associated with the rotation of each group (R) along the N−R α-bond relative to the nitrogen (Figure 4) and NC−R β-bond relative to nitrogen were calculated. This analysis provided plots similar to those used in conformational analyses, as can be seen in Figure 5, plots a and b.

To study the effect of various functional groups, different R substituents were substituted in place of one of the **1a** methyl groups. The structure of **1a** was used as the core structure due to the importance of the cyclohexyl ring systems, and the geometric properties of **1a** are based on X-ray crystal structure data. The alkyl substituents used in this study (Figure 6) can be separated into α, β, γ, and δ depending on the number of carbon atoms extended from the nitrogen center (1, 2, 3, and 4, respectively). The steric hindrance imposed by an alkyl substituent would be expected to increase as the number of carbon atoms (and size of the substituents) increases. However, this effect may be offset by the increase in the rotational degrees

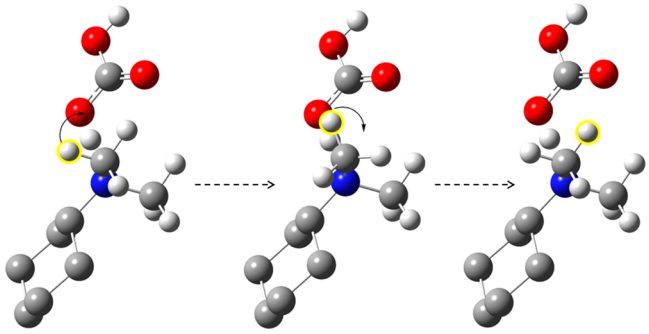

Figure 4. Select PES scan structures for **1a** showing eclipsed and staggered geometries that occur as the methyl hydrogen atoms are rotated by 60° about the N1−C7 α-bond. A single methyl hydrogen atom is highlighted in yellow for clarity.

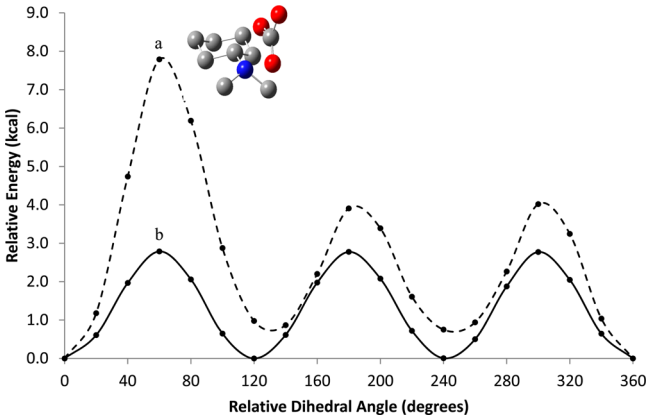

Figure 5. Potential energy surface scans for the C7−N1−C1−C6 (plot a) and C1−N1−C7−H(C7) (plot b) dihedral angles of **1a** (see Figure 2). Both scans are shown but are not comparable as they represent the rotation of two separate dihedral bonds. The figure shows the conformation of the highest energy peak, where it can be seen that the large relative energy is associated with a geometry where both methyl groups eclipse the proximate C−C bonds of the cyclohexyl ring.

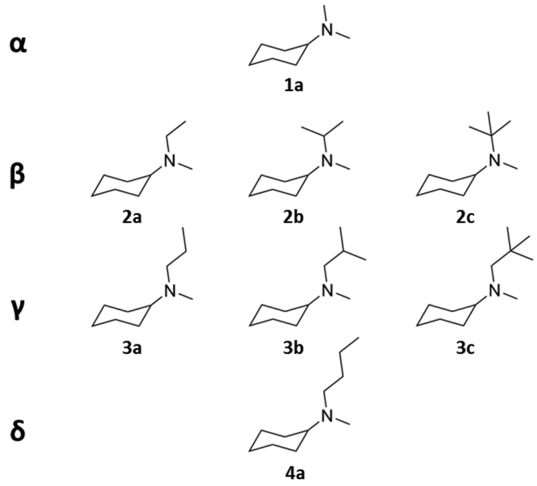

Figure 6. Computational model configurations used in this study.

DOI: 10.1021/acs.jpcb.5b03167
J. Phys. Chem. B 2015, 119, 6766−6775

of freedom as the carbon chain is extended, allowing the group to orient itself away from the nitrogen center, thereby having minimal impact on the reaction of the amine with carbonic acid.

3.4. Functional Group Steric Effects of Base Case 1a. The rotation of the C7-hydrogen atoms along the α-bond (N1−C7) of **1a** gave expected results with three peaks corresponding to the eclipsed geometries (Figure 5). A useful scale to gauge various energies reported in this paper is the energy of a hydrogen bond. A $N-H^{+}\cdots O^{-}$ hydrogen bond is on the order of 7 kcal/mol. Energy peaks significantly larger than 7 kcal/mol where there is a clear interaction between the steric group and the bicarbonate suggest a lower energy state may be accessible in solution by breaking the hydrogen bond and releasing bicarbonate or carbonic acid.

The energies associated with the PES scan of a methyl α-bond (N1−C7) in **1a** can be attributed to the staggered/eclipsed states between functional groups, which has a limited impact on steric hindrance around the nitrogen center. This minimal steric impact can be in part demonstrated through the limited rotation of the bicarbonate ion around its hydrogen bond during the PES scan, Table 4. Comparing the extent to which this bicarbonate rotation takes place for each functional group provides additional insight into each group's steric impact. The rotation of the methyl hydrogen atoms about the α-bond of **1a** (Figure 5, plot b) has a small impact on the C1−N1−O1−O2 dihedral angle (standard deviation from average angle: 2.8) suggesting minimal steric impact as expected (see Table 4 for summary of results).

The rotation of the cyclohexyl group about its α-bond (N1−C1, Figure 5, plot a) provides an energetic profile with a larger average when compared to the rotation of methyl hydrogen atoms (2.5 vs 1.7). As can be seen in Figure 4, rotation of the cyclohexyl group gives a comparatively large barrier of rotation, which is associated with the geometry where the methyl groups are both eclipsing the proximate C−C bonds of the cyclohexyl ring. Despite a larger average energy, the rotation of the cyclohexyl group is similar to the rotation of the methyl in that it has a minimal impact on the position of the bicarbonate group (standard deviation; 2.2). This small effect suggests that the cyclohexyl group does not significantly hinder the interaction of the nitrogen center with a hydrogen atom donor used in the computational model. As discussed, a strong interaction between the polar, ionic pair is a necessary component of the function of an amine as a SPS. The minimal impact of the cyclohexyl group on the ability of this interaction is consistent with experimental observations demonstrating the high SPS performance of dmcha and other cyclohexyl containing amines.

Table 4. Summary of Results Showing Calculated Average Area (Sum of Energies at Each Step Divided by Number of Steps) for the PES Scans of Each Configuration, as Well as the Overall Impact on the Position of the Bicarbonate Group (Average C1−N1−O1−O2 Dihedral Angle, Standard Deviation from Average, and Difference between Maximum and Minimum Angles from Average)[a]

			effect on position of bicarbonate group (deg)		
substituent	av energy (kcal/mol)	barrier of rotation (kcal/mol)	av	std dev	max − min
$\mathbf{1a}_{cy}$	2.5	7.8	179.3	2.2	7.4
$\mathbf{1a}_{H}$	1.7	3.5	178.8	2.8	7.8
2a	2.8	8.8	169.4	9.9	31.5
2b	3.8	9.7	160.4	12.3	39.1
2c	na	na	76.1	71.2	240.1
3a	2.9	9.0	169.4	9.9	28.9
3b	2.8	9.9	163.4	15.8	43.5
3c	na	na	na	na	na
4a	2.8	9.0	169.3	10.4	30.3
$\mathbf{4a}_{\beta}$	2.5	7.6	99.0	46.9	106.2
$\mathbf{3a}_{\beta}$	2.6	7.4	98.7	46.6	104.7
$\mathbf{3b}_{\beta}$	2.7	6.5	85.3	43.8	112.4

[a] $\mathbf{1a}_{cy}$ corresponds to cyclohexyl group rotation, and $\mathbf{1a}_{H}$ corresponds to methyl hydrogen rotation.

3.5. Analysis of Functional Group Steric Effects: PES Scans of the α-Bond in *n*-Alkyl Model Compounds. Relaxed potential energy surface scans were performed along the α-bond (N1−C7) for **2a**, **3a**, and **4a**, and compared to that of **1a**. In all cases, the C1−N1−C7−C10 dihedral angle (Figure 7, plots a, b, and c) was scanned in 20° increments for a full 360° rotation. The SCF energy was calculated at each point, and the relative energy (energy at step n − energy of optimized geometry) was plotted against the number of scan steps (Figure 7).

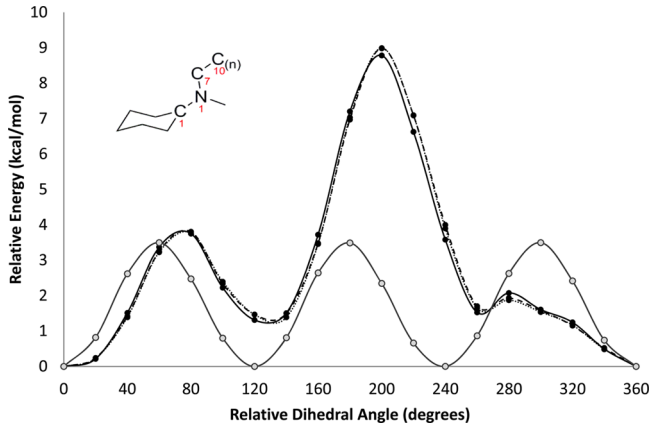

Figure 7. PES scans for C1−N1−C7−R dihedral angle of **2a** (solid, plot a), **3a** (dashed, plot b), and **4a** (dotted, plot c). Each scan step corresponds to a 20° rotation. The PES scan for $\mathbf{1a}_{H}$ (plot d) is shown in gray for comparison.

The lowest energy states for **2a**, **3a**, and **4a** all feature the C7−C10 bond gauche-eclipsed with the N1−O1 hydrogen bond (Figure 8). This indicates that **2a**, **3a**, and **4a** all start in a higher energy state than **1a**, which starts with an enhanced

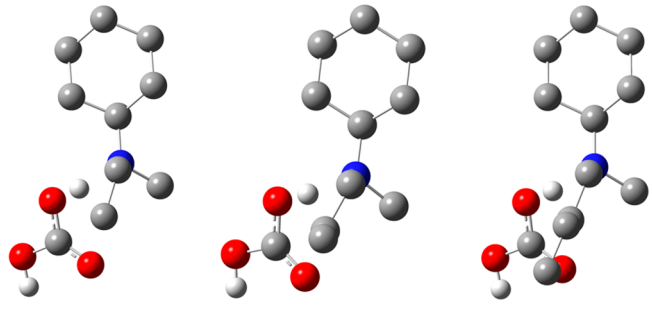

Figure 8. Energy minimized **2a** (left), **3a** (center), and **4a** (right).

DOI: 10.1021/acs.jpcb.5b03167
J. Phys. Chem. B 2015, 119, 6766−6775

overlap between the functional group and the hydrogen bond. This means that the energy values in Table 4 for **1a** are not directly comparable to the energy values for **2a**, **3a**, and **4a**. Nonetheless, the PES scan is extremely informative. It can be seen that the change in energy associated with the rotation of the given substituent is quite similar for **2a**, **3a**, and **4a**, with two dominant peaks in energy. Starting from a gauche-eclipsed state means that eclipsed states are not reached at 60°, 180°, and 300° as is the case with **1a** but rather ∼20° deviated, at 80°, 200°, and 320°. For each configuration, the C7−C10 bond eclipses the N1−methyl bond at 80°, giving rise to a local energy maximum. At 200°, the C7−C10 bond eclipses the N1−C1 bond, providing the highest energy point along the potential energy surface in all three cases. The results also suggest that the rotation of an alkyl chain about the α-bond involves a ∼9 kcal/mol energy barrier and that the length of the carbon chain has minimal impact on the barrier of rotation.

The region where the relative energy is less than that of **1a** is the region where the C7−C10 bond eclipses the hydrogen bond, suggesting minimal steric impact on ion pairing at the nitrogen center resulting from rotation around the α-bond. The eclipsed interactions between the *n*-alkyl chains and the nitrogen's cyclohexyl and methyl substituents in **2a**, **3a**, and **4a** all feature 6 atoms and 5 bonds when the protons are included.

This collection of atoms brings the functional groups into close contact as a pseudo six membered ring with all the steric disruption of a close approach, but without the benefit of the final bond (Figure 9). The eclipsed interaction between the *n*-alkyl chains and the nitrogen's proton only involves 5 atoms and 4 bonds. The pseudo five membered ring conformation results in a significantly smaller steric interaction. What steric bulk the hydrogen bond does have is embodied in the bicarbonate ion, which is free to rotate around the hydrogen bond. The position of the hydrogen-bonded bicarbonate group is disrupted during the PES scan of **2a**, **3a**, and **4a** (Table 4). All three configurations disrupt the position of the bicarbonate group to a similar degree, and to a larger degree than that of **1a**. This indicates that there is some steric impact on the hydrogen bond resulting from rotations along the α-bond with *n*-alkyl substituents.

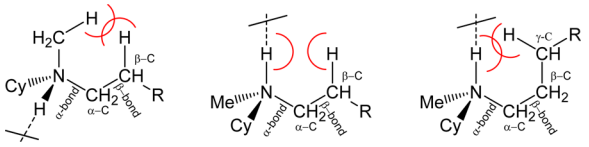

Figure 9. Pseudo six membered ring formed by the nitrogen methyl and R-substituent (left); pseudo five membered ring formed by rotation of the R-substituent around the α-bond into the vicinity of the hydrogen bond (center); and pseudo six membered ring formed by the rotation of the R-substituent around the β-bond into the vicinity of the hydrogen bond (right). Red semicircles depict potential steric hindrance.

3.6. Analysis of Functional Group Steric Effects: PES Scans of the α-Bond in Branched Model Compounds.

The PES scan around the alpha dihedral angle for *n*-alkyl substituents found little to no differences between average energies, barriers of rotation, or displacement of the bicarbonate for any of the *n*-alkyl systems, **2a**, **3a**, and **4a**. Despite the constraints of the α-bond dihedral angle, rotation of each of these alkyl chains could relax in a similar way, giving the minimized structures at each PES scan step very similar relative energies. Experimental results indicate the steric impact of an ethyl, *n*-propyl, and *n*-butyl on the stability of the SPS ion pair is different,[18] which suggests that the α-bond dihedral angle is not the best parameter to consider when investigating these steric effects.

Attempts to prevent the molecule from relaxing by adding branching were not ideal. By including branching at the β or γ position, it was hoped that minimal energy states would be partially disrupted. The PES scans for **2b** and **3b** are shown in Figure 10, plots a and b, with the results summarized in Table 4. The barrier of rotation is slightly larger for **2b** (9.7 kcal/mol) and **3b** (9.9 kcal/mol) than for **2a** (8.8 kcal/mol) and **3a** and **4a** (9.0 kcal/mol). It can be seen in Table 4 that the addition of branched groups does not have a drastic impact on the average relative rotational energy or the barrier of rotation for rotation along the α-bond compared to the unbranched systems. However, there is a slightly larger disturbance of the relative position of the bicarbonate group which is consistent with the expected larger overall steric impact associated with branched groups vs linear alkyl chains.

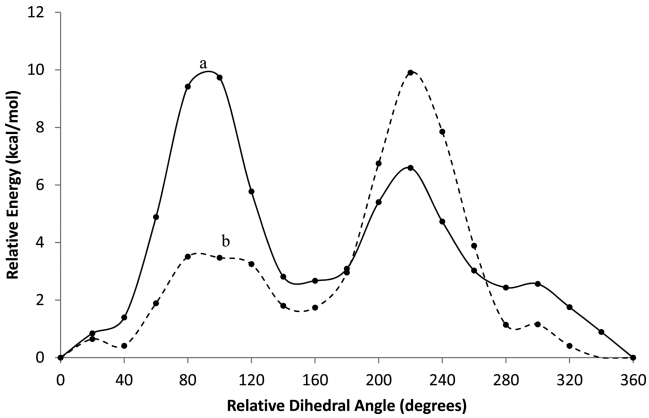

Figure 10. PES scans for the C1−N1−C7−R dihedral angle of **2b** (plot a) and **3b** (plot b). Each scan step corresponds to a 20° rotation.

Taking branching one step further with the addition of two branching points at the β and γ positions, **2c** and **3c** resulted in molecules for which full PES scans could not be completed. The neopentyl substituent, **3c**, provided a geometry that was too bulky for successful optimization; all attempts resulted in atomic rearrangements with irrelevant geometries, so **3c** was not pursued further. Relaxed potential energy surface scans were performed for the α-bond (C1−N1−C7−C10) of **2c**. A full 360° rotation was attempted; however, the scan could not be completed due to large structural changes caused by the rotation of the *tert*-butyl group. The partial scan allows for minimal analysis and no energetic comparison with other configurations. As shown in Table 4, rotation along the α-bond in **2c** forces a dramatic change in the position of the bicarbonate group, which rotates to accommodate the steric bulk associated with the *tert*-butyl substituent. A standard deviation of 71.2° from its average dihedral angle is observed, with a large spread between the maximum and minimum angles (240.1°). As stated, these results are based on a partial scan; however, it seems clear that large structural changes would be needed for cation/anion pairing to take place due to the significant steric hindrance near the nitrogen center associated with the *tert*-butyl group.

DOI: 10.1021/acs.jpcb.5b03167
J. Phys. Chem. B 2015, 119, 6766−6775

These failures in successfully completing PES scans also indicate that branching likely has a more than incremental impact on the sterics around the nitrogen center. In the screening study, there were no tertiary amines with more than two β carbons beyond the dimethyl-*n*-alkylamine core structure without the constraints of a ring system. Hünig's base contains a total of four β carbons beyond the dimethyl-*n*-alkylamine core. Assuming that the sterics associated with these β carbons is more than incremental, Hünig's base would be expected to perform worse than predicted by the initial QSAR model.

3.7. Analysis of Functional Group Steric Effects: PES Scans of β-Bond in Model Compounds. Comparison of the α-bond PES scans for **2a**, **3a**, and **4a** suggests that the difference in steric impact between an ethyl and *n*-butyl group (in terms of their rotational "size") is minimal. The α-bond (C1−N1−C7−C10) dihedral angle represents the only bond rotation of interest for **1a**, **2a**, and **2b**; however, **3a**, **3b**, and **4a** contain more rotational degrees of freedom that need to be considered. Figure 8 shows that for the three configurations, **2a**, **3a**, and **4a**, the R-substituent extends out toward the bicarbonate group in the energy minimized state (a similar geometry is observed for **3b**, though not shown in the figure). Rotation about the β-bond (C7−C10) in **3a**, **3b**, and **4a** would involve the movement of an alkyl group into the vicinity occupied by the bicarbonate. This possibility extends the steric impact of **3a**, **3b**, and **4a** beyond what is represented in the α-bond (C1−N1−C7−C10) PES scans discussed above. To study this potential further, a relaxed PES scan was performed on the β-bond dihedral angle of these three geometries (Figure 11, plots a, b, and c).

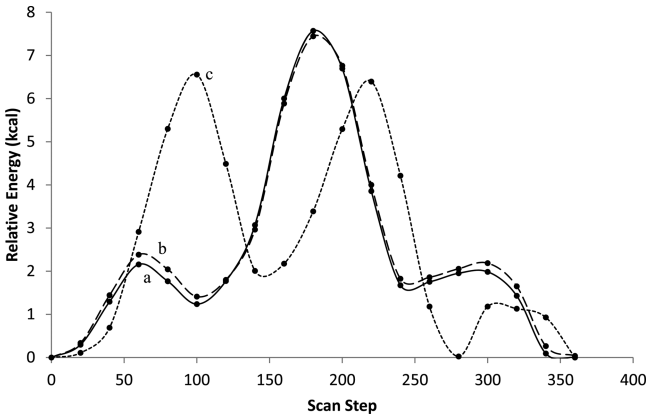

Figure 11. PES scan for the β-bond (N1−C7−C10−C11) dihedral angle of **4a** (plot a), **3a** (plot b), and **3b** (plot c).

As previously stated, the position of the fully relaxed α-bond is gauche-eclipsed with the N1−O1 hydrogen bond (O1−N1−C1−C7 = ~40°) which serves as the initial state for the PES scans of the β-bond dihedral angle. As the rotation takes place, the α-bond remains within ±30° of its initial value relative to the hydrogen bond (O1−N1−C1−C7) through the entire cycle, presumably to avoid overlapping with the other substituents of the tertiary amine. As the β-bond dihedral angle is scanned, the γ carbon is brought within direct contact with the hydrogen bonded bicarbonate group. As the alkyl substituent nears the bicarbonate group during the scan, the α bond generally maintains its relative position so the bicarbonate group is forced into a different orientation to accommodate the steric impact. This geometric change is summarized in Table 4 for the three β scans where the standard deviation and span (max − min) of the dihedral angle associated with the bicarbonate group are large for all three geometries.

As summarized in Table 4 and shown in Figure 11, the average energies and barriers of rotation of the PES scan of the β-bond dihedral angle were not significantly different from the PES α-bond. What is different is that, in the β-bond dihedral angle, the barrier of rotation is associated with interaction between the functional group and the hydrogen bond. In the α-bond dihedral angle the barrier of rotation is associated with interactions between the functional group and the tertiary amine's cyclohexyl group. As noted the α-bond rotation was missing the 6 atoms and 5 bonds required to form a pseudo six membered ring between the hydrogen bond and functional group. In contrast the β-bond rotation features the 6 atoms and 5 bonds required to form a pseudo six membered ring and maximum steric interaction between the hydrogen bond and functional group (Figure 9). Furthermore, the barrier of rotation is between 6.5 and 7.6 kcal/mol despite the freedom of the model complex to freely relax via the α-bond. If the α-bond was constrained to eclipse the hydrogen bond, the barrier would be higher. The 7.6 kcal/mol interaction/barrier of rotation for **4a** is very similar to the energy of a hydrogen bond (N−H$^+$···O$^-$ bond is on the order of 7 kcal/mol). A lower energy state may be accessible in solution by breaking the hydrogen bond.

The β-bond PES scans clearly indicate that this additional rotational degree of freedom increases the potential steric impact of the alkyl substituent. This interaction is in part highlighted by the bicarbonate position changing significantly. The greater steric impact of β-bond rotations supports the initial QSAR model weighting the impact of γ carbons (with β-bond rotations) higher than β carbons, which only have α-bond rotations. In addition, none of the α ring systems have β-bond rotations or equivalent conformational states that would result in the steric bulk of the functional group interacting with the ion pair's hydrogen bond. The ring system's covalent structure constrains its degrees of freedom, reducing their steric impact on the ammonium bicarbonate ion pair. This suggests that, for this ion pair system, the sterics of a cyclohexyl group is less than that of an *n*-propyl group, and possibly less than that of an ethyl group.

3.8. Implications on QSAR Model and Established Steric Parameters. Experiments demonstrated for tertiary amines that steric crowding does not weaken the strength of the hydrogen bond as long as there is a single conformation in which the bond in BH$^+$·B or BH$^+$·H$_2$O can obtain an ideal geometry.[34] This strength refers to the bond dissociation energy (BDE), measured in terms of enthalpy (ΔH). This is easily and well captured in the optimized DFT structures used as our starting point in this study. However, it was also observed that steric crowding may cause entropy effects, as they could hinder internal rotors, which is also supported by our own experimental results and the PES scans conducted in this paper.[18,34] This entropic component (ΔS) contributes to the bond's free energy (ΔG) and equilibrium population (K_{eq}). For the purposes of this study the bond's ΔG and equilibrium concentration are more important than the BDE.

The stability of a transient pair described by an equilibrium constant or corresponding free energy is the product of the free energies of nearly all the possible states (time weighted averaged) found in solution at a given temperature. This by definition includes more than just the minimum energy state found during a conventional DFT calculation. This highlights

DOI: 10.1021/acs.jpcb.5b03167
J. Phys. Chem. B 2015, 119, 6766−6775

the difficulty of using DFT to evaluate something as simple as ion pairing due to the large degree of statistically relevant conformations. For this system, obtaining results consistent with experiment required PES scans around two different dihedral angles, α-bond and β-bond. Luckily the constraints of the system ensured that the α-bond was limited during the β-bond rotation, ensuring that the steric interaction of interest was not missed. While the results of this study support the existing QSAR model, they do not supply results in the form necessary to refine the model or produce another quantitative model. This work also highlights system dependence of steric interactions. Common steric parameters such as Tolman cone angles[35] and Taft values[36,37] both fail to model the steric features important to the SPS ion pair.

4. CONCLUSIONS

An X-ray crystal structure of the *N*,*N*-dimethylcyclohexylammonium bicarbonate (Hdmcha) salt has been solved and reported as an asymmetric unit containing two cation/anion pairs. DFT calculations were used to model the salt and were shown to provide reasonable geometric parameters. Potential energy surface (PES) scans have been performed using the crystallographic data to study the effect of both the length and amount of branching associated with a variety of functional groups on the ability of the groups to disrupt the ion pairing. The barriers of rotation for an α-bond and a β-bond of rotation were found to be similar in energy. However, the barrier of rotation for the α-bond resulted from interactions with the other amine substituent, while the barrier of rotation for the β-bond was a result of direct interactions between the functional group and the bicarbonate ion through a pseudo six membered interaction. The nonlinear impact of branching was also notable, even for α-bond rotations, and provides a reason that Hünig's base is not an effective SPS. The energetic cost and structural impact associated with rotation of larger groups linked to the nitrogen center provide further evidence supporting the use of the QSAR model for explaining SPS behavior. These results are likely relevant to tertiary amine based carbon capture and gas sweetening agents, and an adapted version may likely be applied to secondary and primary amines.

■ ASSOCIATED CONTENT

Supporting Information

The *xyz*-coordinates for all optimized geometries and the crystallographic information file (.cif) for the X-ray crystal structure. The Supporting Information is available free of charge on the ACS Publications website at DOI: 10.1021/acs.jpcb.5b03167.

■ AUTHOR INFORMATION

Corresponding Author

*E-mail: aaron.wilson@inl.gov. Tel: (208) 526-1103.

Notes

The authors declare no competing financial interest.

■ ACKNOWLEDGMENTS

This work was supported by the United States Department of Energy through Contract DE-AC07-05ID14517. Funding was supplied by Idaho National Laboratory via the Laboratory Directed Research and Development Fund (LDRD). Calculations were performed using Idaho National Laboratories High-Performance Computing (HPC) Center. The authors thank Matthew Hartings of American University for useful discussions.

■ REFERENCES

(1) Samorì, C.; Pezzolesi, L.; Barreiro, D. L.; Galletti, P.; Pasteris, A.; Tagliavini, E. Synthesis of New Polyethoxylated Tertiary Amines and Their Use as Switchable Hydrophilicity Solvents. *RSC Adv.* **2014**, *4*, 5999−6008.

(2) Samorì, C.; Barreiro, D. L.; Vet, R.; Pezzolesi, L.; Brilman, D. W. F.; Galletti, P.; Tagliavini, E. Effective Lipid Extraction from Algae Cultures Using Switchable Solvents. *Green Chem.* **2013**, *15*, 353−356.

(3) Samorì, C.; Torri, C.; Samorì, G.; Fabbri, D.; Galletti, P.; Guerrini, F.; Pistocchi, R.; Tagliavini, E. Extraction of Hydrocarbons from Microalga Botryococcus braunii with Switchable Solvents. *Bioresour. Technol.* **2010**, *101*, 3274−3279.

(4) Du, Y.; Schuur, B.; Samorì, C.; Tagliavini, E.; Brilman, D. W. F. Secondary Amines as Switchable Solvents for Lipid Extraction from Non-Broken Microalgae. *Bioresour. Technol.* **2013**, *149*, 253−260.

(5) Boyd, A. R.; Champagne, P.; McGinn, P. J.; MacDougall, K. M.; Melanson, J. E.; Jessop, P. G. Switchable Hydrophilicity Solvents for Lipid Extraction from Microalgae for Biofuel Production. *Bioresour. Technol.* **2012**, *118*, 628−632.

(6) Jessop, P. G.; Kozycz, L.; Rahami, Z. G.; Schoenmakers, D.; Boyd, A. R.; Wechsler, D.; Holland, A. M. Tertiary Amine Solvents Having Switchable Hydrophilicity. *Green Chem.* **2011**, *13*, 619−623.

(7) Holland, A.; Wechsler, D.; Patel, A.; Molloy, B. M.; Boyd, A. R.; Jessop, P. G. Separation of Bitumen from Oil Sands Using a Switchable Hydrophilicity Solvent. *Can. J. Chem.* **2012**, *90*, 805−810.

(8) Zhang, Q.; Oztekin, N. S.; Barrault, J.; De Oliveira Vigier, K.; Jérôme, F. Activation of Microcrystalline Cellulose in a CO2-Based Switchable System. *ChemSusChem* **2013**, *6*, 593−596.

(9) Anugwom, I.; Eta, V.; Virtanen, P.; Mäki-Arvela, P.; Hedenström, M.; Hummel, M.; Sixta, H.; Mikkola, J.-P. Switchable Ionic Liquids as Delignification Solvents for Lignocellulosic Materials. *ChemSusChem* **2014**, *7*, 1170−1176.

(10) Fu, D.; Farag, S.; Chaouki, J.; Jessop, P. G. Extraction of Phenols from Lignin Microwave-Pyrolysis Oil Using a Switchable Hydrophilicity Solvent. *Bioresour. Technol.* **2014**, *154*, 101−108.

(11) Agar, D.; Tan, Y.; Hui, Z. *Separating CO2 from Gas Mixtures*; PCT/EP2007/057907, February 8, 2008.

(12) Zhang, J.; Chen, J.; Misch, R.; Agar, D. W. Carbon Dioxide Absorption in Biphasic Amine Solvents with Enhanced Low Temperature Solvent Regeneration. *Chem. Eng. Trans.* **2010**, *21*, 169−174.

(13) Zhang, J.; Misch, R.; Tan, Y.; Agar, D. W. Novel Thermomorphic Biphasic Amine Solvents for CO2 Absorption and Low-Temperature Extractive Regeneration. *Chem. Eng. Technol.* **2011**, *34*, 1481−1489.

(14) Zhang, J.; Agar, D. W.; Zhang, X.; Geuzebroek, F. CO2 Absorption in Biphasic Solvents with Enhanced Low Temperature Solvent Regeneration. *Energy Procedia* **2011**, *4*, 67−74.

(15) Zhang, J.; Qiao, Y.; Agar, D. W. Improvement of Lipophilic-Amine-Based Thermomorphic Biphasic Solvent for Energy-Efficient Carbon Capture. *Energy Procedia* **2012**, *23*, 92−101.

(16) Zhang, J.; Qiao, Y.; Agar, D. W. Intensification of Low Temperature Thermomorphic Biphasic Amine Solvent Regeneration for CO2 Capture. *Chem. Eng. Res. Des.* **2012**, *90*, 743−749.

(17) Stone, M. L.; Wilson, A. D.; Harrup, M. K.; Stewart, F. F. An Initial Study of Hexavalent Phosphazene Salts as Draw Solutes in Forward Osmosis. *Desalination* **2013**, *312*, 130−136.

(18) Wilson, A. D.; Stewart, F. F. Structure−function Study of Tertiary Amines as Switchable Polarity Solvents. *RSC Adv.* **2014**, *4*, 11039−11049.

(19) Wilson, A. D.; Orme, C. J. Concentration Dependent Speciation and Mass Transport Properties of Switchable Polarity Solvents. *RSC Adv.* **2015**, *5*, 7740−7751.

DOI: 10.1021/acs.jpcb.5b03167
J. Phys. Chem. B 2015, 119, 6766−6775

(20) Stone, M. L.; Rae, C.; Stewart, F. F.; Wilson, A. D. Switchable Polarity Solvents as Draw Solutes for Forward Osmosis. *Desalination* **2013**, *312*, 124−129.
(21) Durelle, J.; Vanderveen, J. R.; Jessop, P. G. Modelling the Behaviour of Switchable-Hydrophilicity Solvents. *Phys. Chem. Chem. Phys.* **2014**, *16*, 5270−5275.
(22) Durelle, J.; Vanderveen, J. R.; Quan, Y.; Chalifoux, C. B.; Kostin, J. E.; Jessop, P. G. Extending the Range of Switchable-Hydrophilicity Solvents. *Phys. Chem. Chem. Phys.* **2015**, *17*, 5308−5313.
(23) Frisch, M.; Trucks, G.; Schlegel, H.; Scuseria, G.; Robb, M.; Cheeseman, J.; Montgomery, J.; Vreven, T.; Kudin, K.; Burant, J.; et al. *Gaussian 03, Revision C.02*; Gaussian, Inc.: Wallingford, CT, 2004.
(24) Vosko, S. H.; Wilk, L.; Nusair, M. Accurate Spin-Dependent Electron Liquid Correlation Energies for Local Spin Density Calculations: A Critical Analysis. *Can. J. Phys.* **1980**, *58*, 1200−1211.
(25) Becke, A. D. Density-Functional Exchange-Energy Approximation with Correct Asymptotic Behavior. *Phys. Rev. A* **1988**, *38*, 3098−3100.
(26) Becke, A. D. Density-functional Thermochemistry. III. The Role of Exact Exchange. *J. Chem. Phys.* **1993**, *98*, 5648−5652.
(27) Becke, A. D. Density-functional Thermochemistry. II. The Effect of the Perdew−Wang Generalized-gradient Correlation Correction. *J. Chem. Phys.* **1992**, *97*, 9173−9177.
(28) Becke, A. D. Density-functional Thermochemistry. I. The Effect of the Exchange-only Gradient Correction. *J. Chem. Phys.* **1992**, *96*, 2155−2160.
(29) Lee, C.; Yang, W.; Parr, R. G. Development of the Colle-Salvetti Correlation-Energy Formula into a Functional of the Electron Density. *Phys. Rev. B* **1988**, *37*, 785−789.
(30) Wilson, A. D.; Stewart, F. F. Deriving Osmotic Pressures of Draw Solutes Used in Osmotically Driven Membrane Processes. *J. Membr. Sci.* **2013**, *431*, 205−211.
(31) Zavitsas, A. A. Properties of Water Solutions of Electrolytes and Nonelectrolytes. *J. Phys. Chem. B* **2001**, *105*, 7805−7817.
(32) Fumino, K.; Fossog, V.; Stange, P.; Paschek, D.; Hempelmann, R.; Ludwig, R. Controlling the Subtle Energy Balance in Protic Ionic Liquids: Dispersion Forces Compete with Hydrogen Bonds. *Angew. Chem., Int. Ed.* **2015**, *54*, 2792−2795.
(33) Meot-Ner (Mautner), M. Update 1 of: Strong Ionic Hydrogen Bonds. *Chem. Rev.* **2012**, *112*, PR22−PR103.
(34) Meot-Ner, M.; Sieck, L. W. The Ionic Hydrogen Bond. 1. Sterically Hindered Bonds. Solvation and Clustering of Protonated Amines and Pyridines. *J. Am. Chem. Soc.* **1983**, *105*, 2956−2961.
(35) Tolman, C. A. Steric Effects of Phosphorus Ligands in Organometallic Chemistry and Homogeneous Catalysis. *Chem. Rev.* **1977**, *77*, 313−348.
(36) Streitwieser, A. The Application of Taft's Equation to Polar Effects in Solvolyses. *J. Am. Chem. Soc.* **1956**, *78*, 4935−4938.
(37) Taft, R. W. Linear Free Energy Relationships from Rates of Esterification and Hydrolysis of Aliphatic and Ortho-Substituted Benzoate Esters. *J. Am. Chem. Soc.* **1952**, *74*, 2729−2732.

DOI: 10.1021/acs.jpcb.5b03167
J. Phys. Chem. B 2015, 119, 6766−6775